



ИНСТИТУТ ЯДЕРНОЙ ФИЗИКИ СО АН СССР

**A.D.Bukin, I.B.Vasserman, P.V.Vorobyov, V.B.Golubev,
V.P.Druzhinin, P.M.Ivanov, V.N.Ivanchenko,
G.Ya.Kezerashvili, A.N.Kirpotin, I.A.Koop, A.P.Lysenko,
E.A.Perevedentsev, A.N.Peryshkin, A.A.Polunin,
I.Yu.Redko, S.I.Serednyakov, V.A.Sidorov, A.N.Skrinsky,
Yu.V.Usov, Yu.M.Shatunov, S.I.Eicelman**

**PRELIMINARY RESULTS FROM
THE NEUTRAL DETECTOR AT VEPP-2M**

ПРЕПРИНТ 83—80



НОВОСИБИРСК

Abstract

Preliminary results of experiments with the neutral detector at the electron-positron storage ring VEPP-2M are presented. Branching ratios of the Φ -meson radiative decays have been measured:

$$B(\Phi \rightarrow \eta\gamma) = (1.14 \pm 0.11)\%,$$

$$B(\Phi \rightarrow \pi^0\gamma) = (0.11 \pm 0.03)\%.$$

Upper limits at the 90% confidence level have been obtained for the following Φ -meson decays:

$$B(\Phi \rightarrow \eta e^+e^-) < 6 \cdot 10^{-4},$$

$$B(\Phi \rightarrow X_1\gamma) < 2 \cdot 10^{-5},$$

where X_1 is a light boson with a mass less than 200 MeV undetected by the neutral detector,

$$B(\Phi \rightarrow X_2\gamma) < 2 \cdot 10^{-3},$$

where X_2 is a light boson with a lifetime less than 10^{-11} sec and a mass less than 10 MeV decaying into 2 photons. A process of Compton scattering of quasireal photons by electrons and positrons has been studied in detail.

Introduction

This work starts a series of publications presenting results of experiments with the neutral detector (ND) at the electron-positron storage ring VEPP-2M [1]. The neutral detector [2] shown in fig.1 is a calorimeter of γ -quanta and electrons based on 168 rectangular scintillation counters with NaI(Tl) crystals [3] (total weight about 2.6 tons). Two layers of two-coordinate shower proportional chambers to measure photon angles are installed inside the calorimeter. In the detector centre there is a tracking system for charged particles consisting of three layers of cylindrical proportional chambers [4]. To suppress a background due to cosmic particles anticoincidence scintillation counters have been installed outside the detector separated from NaI(Tl) crystals by an iron absorber 10 cm thick. A total solid angle of the detector is about 65% of 4π steradian. The energy calibration of the detector is performed by cosmic muons using a special trigger. The energy resolution is determined by the amount of «passive» material between NaI(Tl) crystals (walls of NaI(Tl) counters, material of shower chambers, etc.) and for photons in the energy range $50 \div 1000$ MeV is $25 \div 10\%$ (FWHM). The angular resolution for photons is 2 degrees (RMS) in an azimuthal direction and 4 degrees (RMS) for a polar angle.

The experiment has been performed in the C.M. energy range from 1000 to 1048 MeV with an average luminosity of $0.7 \cdot 10^{30} \text{cm}^{-2} \text{sec}^{-1}$. The cited energy range was scanned several times with a step of 0.5 MeV. The integrated luminosity in the experiment was 2.7pb^{-1} , about 13 millions events were recorded, 3 millions of them being Φ -meson decays. The luminosity monitoring during the data taking was performed by a double bremsstrahlung, the final normalization during data processing was based on the events of Bhabha scattering and two-quantum annihilation at large angles and had a 3% accuracy. About 6 millions events of these reactions were recorded. The energy scale of the storage ring was calibrated using the table value of the Φ -meson mass [5]. The excitation curve for neutral decays of the Φ -meson is shown in Fig.2. The value of the observed cross section is determined with a 10% accuracy by the decay mode $\Phi \rightarrow K_S K_L$ neutrals. Up to now about half of the recorded information has been processed corresponding to the integrated luminosity of 1.5pb^{-1} .

Radiative Decays of Φ -Meson

Up to now the most accurate measurements of the Φ -meson radiative decays have been performed at the colliding beams [6] and in photoproduction experiments [7]. This work presents preliminary results on the investigation of the reactions

$$\Phi \rightarrow \eta \gamma \rightarrow 3\gamma \quad (1)$$

$$\Phi \rightarrow \pi^0 \gamma \rightarrow 3\gamma \quad (2)$$

The fact that recoil photons in these reactions are monochromatic allows separation of these reactions as well as the background processes

$$e^+e^- \rightarrow 3\gamma \quad (\text{QED}) \quad (3)$$

$$\Phi \rightarrow K_S K_L \quad \text{neutrals} \quad (4)$$

For the preliminary selection of three-photon events the following conditions have been used:

- there are no tracks in coordinate chambers,
- each photon triggers a shower chamber,
- total energy deposition in the detector exceeds 600 MeV.

2933 events thus selected have been subjected to a kinematical reconstruction [8]. In this procedure energy-momentum conservation is used to determine with a better accuracy particle energies and angles measured in the detector as well as to improve a resolution in an effective mass of η and π^0 -mesons (Fig.3). Events not satisfying conservation laws are rejected completely eliminating a background due to the process (4). A part of 1245 selected events is shown in Fig.4 together with the distributions for the processes (1), (2) and (3) obtained by Monte Carlo simulation.

The detection cross section for each of the processes can be written as

$$\sigma(E) = \varepsilon \alpha(E) \sigma_0(E) + \sigma_b(E);$$

where $\sigma_0(E)$ is a cross section in the first Born approximation, $\alpha(E)$ is a factor taking into account radiative corrections [9], $\sigma_b(E) = \text{const}/E^2$ is a cross section of background processes, ε is a detection efficiency calculated by the Monte Carlo method [10]. The following expression for the cross section has been used:

$$\sigma_0(E) = \sigma_0^{\text{max}} [(1 - M_p^2/4E^2)/(1 - M_p^2/M_\Phi^2)]^3 \Gamma_\Phi^2/M_\Phi^2 |A + [1/(1 - 4E^2/M_\Phi^2 + i\Gamma_\Phi/M_\Phi)]|^2$$

where σ_0^{max} is a cross section in the Φ -meson maximum, M_p is a η or π^0 mass, A is a non-resonant interfering amplitude determined by a contribution of ρ and ω -mesons.

For the process $e^+e^- \rightarrow 3\gamma$ (QED) a fit of the measured cross section gave results consistent with a simulation prediction. This process determines completely a non-resonant part of the cross section $\sigma_b(E)$ for radiative decays (1) and (2). The contribution of the reaction (4) is negligibly small for all investigated processes.

Fixing a mass and a width of the Φ -meson and assuming $A=0$, one can obtain the following values of total cross sections for the reaction (1)

$$\sigma_0^{\text{max}} = (19.6 \pm 1.1 \pm 1.5) \text{ nb}$$

$$\sigma_b = (0.10 \pm 0.02) \text{ nb}$$

and for the reaction (2)

$$\sigma_0^{\text{max}} = (4.6 \pm 0.9 \pm 0.7) \text{ nb}$$

$$\sigma_b = (0.034 \pm 0.008) \text{ nb}$$

Optimum excitation curves of the Φ -meson are shown in Fig.5 and are consistent with the assumption of the absence of the interfering amplitude. The first error of the values above is statistical, while a second one systematical. The latter is estimated to be 6% and is determined by the following factors: the accuracy in the detection efficiency calculation, the accuracy of the absolute luminosity determination as well as that of radiative corrections. Using table values [5]

$$B(\eta \rightarrow \gamma\gamma) = (39.1 \pm 0.8) \%$$

$$B(\pi^0 \rightarrow \gamma\gamma) = 98.8\%$$

$$B(\Phi \rightarrow e^+e^-) = (3.11 \pm 0.10) \cdot 10^{-4}$$

$$\Gamma_\Phi = (4.21 \pm 0.13) \text{ MeV}$$

one can obtain

$$\sigma(e^+e^- \rightarrow \Phi \rightarrow \eta\gamma) = (50.0 \pm 2.8 \pm 3.8) \text{ nb}$$

$$\sigma(e^+e^- \rightarrow \Phi \rightarrow \pi^0\gamma) = (4.7 \pm 0.9 \pm 0.7) \text{ nb}$$

$$B(\Phi \rightarrow \eta\gamma) = (1.14 \pm 0.06 \pm 0.09) \%$$

$$B(\Phi \rightarrow \pi^0\gamma) = (0.11 \pm 0.02 \pm 0.015) \%$$

$$\Gamma(\Phi \rightarrow \eta\gamma) = (47.9 \pm 2.7 \pm 3.6) \text{ keV}$$

$$\Gamma(\Phi \rightarrow \pi^0\gamma) = (4.5 \pm 0.9 \pm 0.7) \text{ keV}$$

The errors of the table values were not included in these results which are preliminary since the accuracy can be improved. In particular, a statistical error can be diminished when the number of events in experiment and simulation is increased (presented results are based on a half of the recorded information). With the increase of statistics the measurement of an interfering amplitude becomes possible.

The value found for the decay width $\Phi \rightarrow \eta\gamma$ is by 1.5 standard deviations less than a world-average one and has a smaller error. This result contradicts to the models of SU(3) and nonet symmetry [11,13] ($\Gamma = 135 \pm 10$ keV) and is in much better agreement with the prediction of the effective quark model [12,13] ($\Gamma = 57$ keV).

The decay mode $\Phi \rightarrow \eta\gamma$ has been also studied in the channel $\eta \rightarrow 3\pi^0$. To this end events with 6 or 7 photons were selected. The energy spectrum of a photon with a maximum energy is shown for these events in Fig.6. The left side events are due to the decay $\Phi \rightarrow K_S K_L \rightarrow$ neutrals. The peak at 360 MeV corresponds to the recoil photons of the reaction $\Phi \rightarrow \eta\gamma$. The detection efficiency for this process is $(1.1 \pm 0.3)\%$. 87 events found in the experiment correspond to a branching ratio $B(\Phi \rightarrow \eta\gamma) = (1.8 \pm 0.6)\%$.

Search for $\Phi \rightarrow \eta e^+ e^-$ Decay

Search for the decay $\Phi \rightarrow \eta e^+ e^-$ is interesting since it allows to study a transition $\Phi \rightarrow \eta\gamma^*$, where γ^* is a virtual photon with a mass $q^2 = m_{ee}^2 > 4m_e^2$. The probability of this decay is connected with the probability $\Phi \rightarrow \eta\gamma$ by the following approximate relation

$$\frac{B(\Phi \rightarrow \eta e e)}{B(\Phi \rightarrow \eta\gamma)} \approx \frac{2\alpha}{3\pi} \ln \frac{M_\Phi - M_\eta}{2m} \approx 1\% \quad (5)$$

Formula (5) has been derived from a more accurate formula of Ref.14:

$$\frac{d}{dm_{ee}^2} \left(\frac{B(\Phi \rightarrow \eta e e)}{B(\Phi \rightarrow \eta\gamma)} \right) = \frac{\alpha}{3\pi} \frac{|F(m_{ee}^2)|^2}{m_{ee}^2} \left(1 + \frac{2m^2}{m_{ee}^2} \right) \left(1 - \frac{4m^2}{m_{ee}^2} \right)^{1/2} \times \\ \times \left[\left(1 - \frac{4m_{ee}^2}{M_\Phi^2 - M_\eta^2} \right)^2 - \frac{4M_\eta^2 m_{ee}^2}{(M_\Phi^2 - M_\eta^2)^2} \right]^{3/2}$$

where $F(m_{ee}^2)$ is a transition form factor significant large contribution at $m_{ee} \gtrsim 200$ MeV. The main contribution to the decay $\Phi \rightarrow \eta e^+ e^-$ is

given by a region of m_{ee} close to a threshold $m_{ee} \gtrsim 2m_e$ therefore to derive (5) a form factor was taken to be 1.

To search for this decay events were selected with 2 charged particles and 2 photons satisfying energy-momentum conservation and a total energy deposition greater than 600 MeV. Energy-momentum conservation was checked by a kinematical reconstruction method similar to that described in the previous section. An additional condition required that an angle between a charged particle and a photon be greater than 30 degrees.

The same final state can appear in the decay $\Phi \rightarrow \eta\gamma$, $\eta \rightarrow e^+ e^- \gamma$ in which one of the photons is monochromatic with an energy about 360 MeV and in the non-resonant process of double bremsstrahlung (DB) at large angles. It is convenient to analyze these processes by means of a two-dimensional plot of Fig.7. Its vertical axis shows an effective mass of the photon pair, while a horizontal axis depicts a photon energy closest to that of the recoil photon in the decay $\Phi \rightarrow \eta\gamma$, $\eta \rightarrow e^+ e^- \gamma$. A characteristic feature of the process under study is the constancy of the effective mass of the photon pair. Results of the Monte Carlo simulation of these processes are shown in Fig.7a, the calculated detection efficiency is $(1.5 \pm 0.4)\%$. Total number of events in the experiment was 12. They are shown in Fig.7 from which one can see that 4 events can be ascribed to the decay $\Phi \rightarrow \eta\gamma$, $\eta \rightarrow e^+ e^- \gamma$ whereas one expects 1.7 events and about one event due to DB. 2 events are found in the region of the decay $\Phi \rightarrow \eta e^+ e^-$, $\eta \rightarrow 2\gamma$ corresponding to a branching ratio of $(2.2 \pm 1.8) \cdot 10^{-4}$. The rest of events in Fig.7 have continuous distribution and are probably due to DB. Their number agrees with a qualitative estimation. Since no detailed calculation of DB is available at the present time and taking into account a smallness of the number of experimental events, one can't determine a contribution of DB to the region of the decay $\Phi \rightarrow \eta e^+ e^-$. Therefore as a result we present an upper limit for this decay which at the 90% confidence level is $B(\Phi \rightarrow \eta e^+ e^-) < 6 \cdot 10^{-4}$.

An increase of the experimental statistics by one order of magnitude will allow a reliable determination of the branching ratio. To investigate a transition form factor in the accessible range of $m_{ee} < 470$ MeV one needs an increase in the number of events by a factor of about 100.

Search for the Process $e^+e^- \rightarrow X + \gamma$

Recently a problem of the existence of new light bosons was actively discussed, for example, an axion [15] or a supersymmetric boson [16] and their experimental search has been performed. In our work we looked for events of a hypothetical reaction $e^+e^- \rightarrow X_1 + \gamma$ where X_1 is a boson of such a type with a mass not greater than 200 MeV. It was assumed that neither this boson nor its decay products are detected by ND. For analysis events were selected with one photon coming from an interaction point triggering two layers of shower chambers and three layers of NaI(Tl) with a threshold of 5 MeV. The detection efficiency for photons with an angular distribution $dN = (1 + \cos^2\theta) d\theta$ obtained by the Monte Carlo simulation is $(17 \pm 1)\%$.

An energy spectrum of 1163 events thus selected is shown in Fig.8. An insertion to the figure shows an expected spectrum for photons with a beam energy and 13% resolution (FWHM). 35 events have been found within these boundaries in a hard part of the spectrum. The energy dependence of their detection cross section depicted in Fig.9 does not give evidence for some increase in the Φ -meson region.

The events found are mostly synchronized with a beam by the time of the detector trigger and possess a flat distribution in the interaction point along the beams. This is an indication that the main source of such events (with the exception of a hard part of the spectrum) is a process of bremsstrahlung at large angles due to a residual gas in a vacuum chamber. Results of the «background» runs when beams collided in another interaction region are in consistence with this assumption. It is also confirmed by numerical estimation of the number of events at the pressure of the residual gas of 10^{-8} torr. Besides the bremsstrahlung process connected with a residual gas a 10% contribution is given by the bremsstrahlung of electrons on positrons and by triggers due to cosmic particles.

As to the hard part of the spectrum (Fig.8), the main contribution comes from the process of three-quantum annihilation in which only one photon is detected. The Monte Carlo simulation of this reaction has not yet been done, however, estimations gave the number of events close to the observed one.

The energy dependence of the detection cross section (Fig.9) is consistent with being constant (χ^2 equals 6.1 at 9 degrees of freedom) and corresponds to a value of the detection cross section (23 ± 4) pb

(an error is statistical) or to a total cross section 130 ± 20 pb. Since no quantitative subtraction of the background due to three-quantum annihilation has been performed, one must consider this result as an upper limit on the cross section of the reaction $\sigma(e^+e^- \rightarrow X_1 + \gamma) < 160$ pb in the energy region $1000 \div 1048$ MeV at 90% confidence level. The absence of a peak in Fig.9 in the Φ -meson region allows to establish an upper limit for the decay $B(\Phi \rightarrow X_1 + \gamma) < 2 \cdot 10^{-5}$ (90% c.l.) Our value is very close to an upper limit for a similar decay of the Ψ -meson produced by the Crystal Ball group [17].

If a hypothetical particle X_2 decays into two photons with a small lifetime $\tau < 10^{-11}$ sec and has a small mass $M(X_2) < 10$ MeV, a final state will be $e^+e^- \rightarrow X_2 + \gamma \rightarrow 3\gamma$. An angle between decay photons is very small ($\alpha < 1^\circ$), therefore photons merge into one photon in ND and such event is undistinguishable from that of two-quantum annihilation. Thus the decay $\Phi \rightarrow X_2 + \gamma$ will reveal itself as a peak in the cross section of two-quantum annihilation at $2E = M_\Phi$. The cross section observed in the experiment is presented in Fig.10. One can see that within several per cent accuracy no peak is observed in the Φ -meson region. The detection efficiency in this case is $(25 \pm 4)\%$ giving after a fit a value $B(\Phi \rightarrow X_2 + \gamma \rightarrow 3\gamma) < 2 \cdot 10^{-3}$ at 90% c.l.

Test of Quantum Electrodynamics in Compton Scattering of Quasireal Photon by Electron

One of the first processes identified in experiments with ND was that of Compton scattering of a quasireal photon by a colliding electron. This reaction has first been observed in experiments at the ACO collider in 1973 [18] with the total number of events less than 20. The integrated luminosity of our experiment allows to increase considerably this number and perform a detailed study of the reaction.

The process under study is described by diagrams of Fig.11 and is a particular case of single bremsstrahlung when a virtual photon with an energy close to that of a beam is near a mass shell $q_\gamma^2 \simeq -m_e^2$. Its kinematics is rather simple: one of the initial particles is scattered by an angle $\alpha \sim 1/\gamma$ and escapes detection while another electron and a photon fly at large angles. Let us refer to this process as virtual Compton scattering (VCS). Its theory in Weizsacker-Williams approximation was developed in [19], a more detailed expression for the cross section was presented in Ref.20. Investigation of VCS allows a test of QED with e^+e^- -colliding beams in a region where the cross

section is determined by an electron propagator at positive q_e^2 . This region differs from those in standard QED tests by e^+e^- elastic scattering, production of $\mu^+\mu^-$ and two-photon annihilation. Also of interest in this reaction is the possibility to look for a heavy electron [21] which must reveal itself as a peak in a distribution of invariant masses of one final electron and a photon. Recently such a search at $q_e^2 \lesssim 1 \text{ GeV}^2$ has been performed with the OLYA detector at VEPP-2M collider [22]. An additional peculiarity of the VCS is a possibility of unambiguous determination which of the initial particles scatters a photon, i.e. to compare directly VCS for an electron and positron.

To study VCS the data of two first scannings corresponding to the integrated luminosity of 800 nb^{-1} has been used. Events were selected with one charged particle and one photon having an energy deposition greater than 400 MeV. These events contain these of VCS as well as background events of the two types: the two-photon annihilation with the conversion of one photon in front of the coordinate chambers and these due to hadronic decays of the Φ -meson. To suppress this background events with an acollinearity angle greater than 10° and a acoplanarity angle less than 10° were selected. Special method using the information on energy deposition in NaI(Tl) layers allowed to discriminate electrons and pions. Rejecting events with pions we obtained 4796 events due to VCS. The energy dependence of the observed cross section is presented in Fig.13. One observes no peak in the region of the Φ -meson.

Comparison of the experimental results with theoretical predictions was performed both by an observed cross section and by angular and energy characteristics. The theory predictions were obtained by the Monte Carlo simulation of the following formula from Ref.20:

$$d\sigma = d\sigma_a + d\sigma_b$$

$$d\sigma_a = \alpha^3/E^2 [d\cos \theta_\gamma / (1 - \cos \theta_\gamma)^2] (d\xi/\xi) \ln (E/m\xi) [(1 + \eta^2) [(1 - \xi)^2 + \eta^2] / \eta^2] \quad (6)$$

$$d\sigma_b = d\sigma_a(-\cos \theta_\gamma); \quad \xi = E_\gamma/E; \quad \eta = 1 - (1 + \cos \theta) \cdot \xi/2;$$

The accuracy of (6) is about 10%. The calculated detection cross section is $6.60 \pm 0.16 \text{ nb}$ (an error is statistical), while the experimental value is $6.0 \pm 0.3 \text{ nb}$ (an error is systematical). One can ascribe the observed difference in these values to an accuracy of formula (6).

The following distributions confirm that the process observed is really Compton effect:

- 1) acollinearity angle between an electron and a photon,
- 2) transverse momentum of a system electron+photon,
- 3) effective mass of a virtual photon.

All these distributions (Figs.14,15) have a narrow peak near zero with a width determined by the process properties and an apparatus resolution of ND. The distributions in the polar angle of electron and photon presented in Fig.16 also demonstrate good agreement between experiment and theory.

An important dynamical characteristics of VCS is a spectrum of invariant masses of electron and photon usually serving to check QED (see Fig.17). No significant deviations from theory are observed implying that QED is valid in the process under study and no heavy electrons are produced. To obtain quantitative characteristics of QED validity as well as restrictions on heavy electron parameters we are going to perform VCS simulation using exact QED formulae.

The total detection cross sections of VCS by an electron and positron coincide within a 2% accuracy (the error is statistical), the angular distributions of Fig.18 also do not show statistically significant differences. These results test C-invariance in photon scattering by electrons and positrons.

In conclusion the authors express their profound gratitude to E.A.Kuraev and G.N.Shestakov for useful discussions.

References

1. *G.M.Tumaikin*, Proc. of 10 International Conf. on High Energy Accelerators, V.1, p.443, Serpukhov, 1977.
2. *V.M.Aulchenko et al.*, Preprint INP 82-112, Novosibirsk, 1982.
3. *M.D.Minakov et al.*, Pribory i Tekhnika Experimenta, 4, (1980)558.
4. *V.B.Golubev et al.*, Pribory i Tekhnika Experimenta, 6, (1981)40.
5. Review of Particle Properties, Particle Data Group, 1982.
6. *G.Cosme et al.*, Phys. Lett. 63B(1976)352.
7. *D.E.Andrews et al.*, Phys. Rev. Lett. 38(1977)198.
8. *J.Berge et al.*, Rev. Sci. Instr. 32(1961)538.
9. *J.D.Jackson and D.L.Sharre*, Nucl. Instr. Meth. 128 (1975)13.
10. *A.D.Bukin and S.I.Eidelman*, Preprint INP 77-101, Novosibirsk, 1977.
11. *T.Oshima*, Phys. Rev. D22(1980)707.
12. *D.A.Geffen and W.Wilson*, Phys. Rev. Lett. 44(1980)370.
13. *P.J.O'Donnell*, Rev. Mod. Phys. 53(1981)673.
14. *C.H.Lai and G.Quigg*, Preprint FN-296, Fermilab, 1976, *R.I.Dzhelyadin et al.*, Phys. Lett. 102B(1981)296.
15. *W.A.Bardeen et al.*, Phys. Lett. 76B(1978)580.
16. *P.Fayet and M.Mezard*, Phys. Lett. 104B(1981)226.
17. *C.Edwards et al.*, Phys. Rev. Lett. 48(1982)903.
18. *G.Cosme et al.*, Lett. Nuovo Cim. 8(1973)560.
19. *G.Carimalo et al.*, Nucl. Phys. B57(1973)582.
20. *V.N.Baier et al.*, Phys. Rep. 78(1981)2.
21. *F.E.Low*, Phys. Rev. Lett. 14(1965)238.
22. *A.D.Bukin et al.*, Yadernaya Fizika 35(1982)1444.

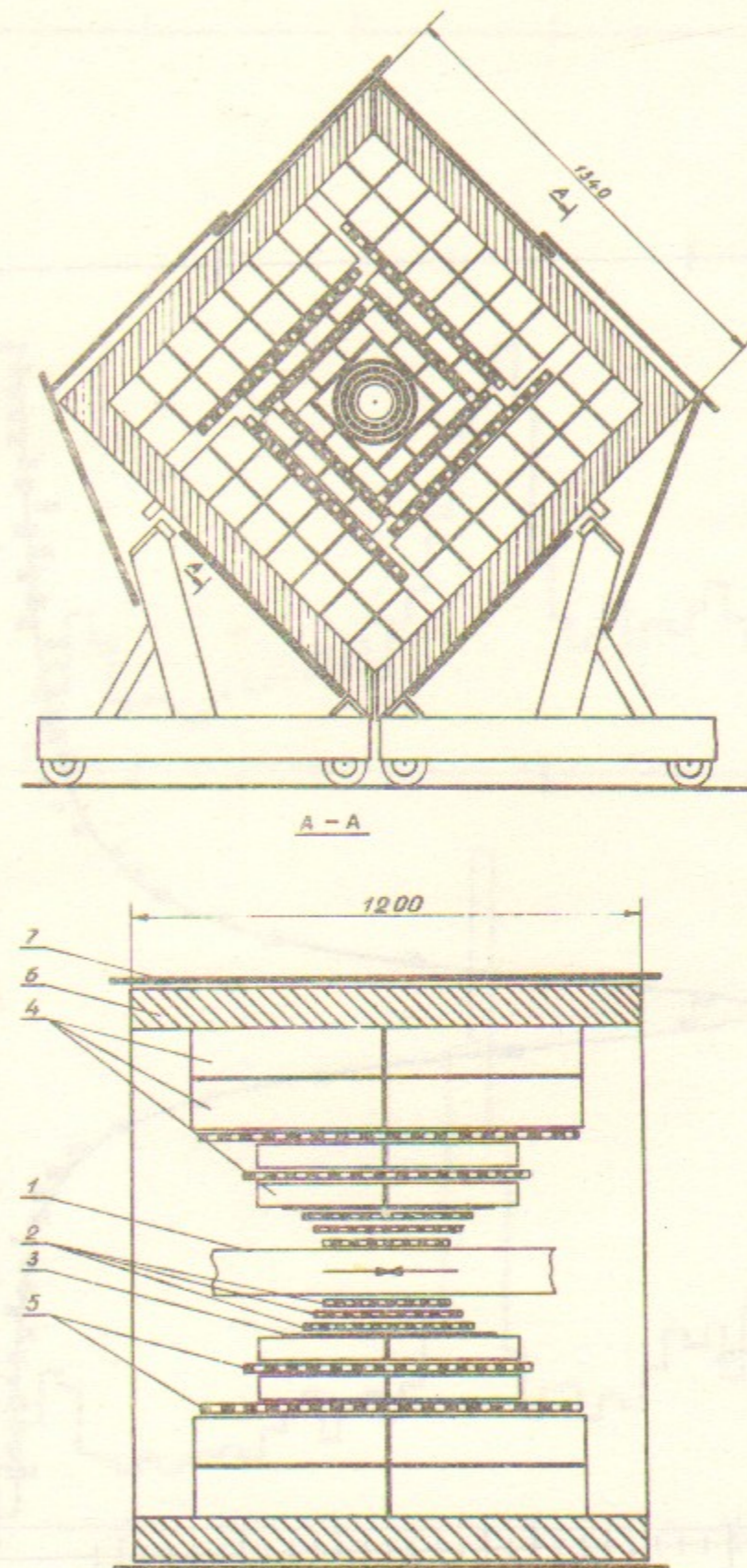


Fig.1. Lay-out of the neutral detector: 1—vacuum chamber of the storage ring, 2—coordinate proportional chambers, 3—scintillation counters, 4—NaI(Tl) counters, 5—shower chambers, 6—absorber (10 cm iron), 7—anticoincidence counters.

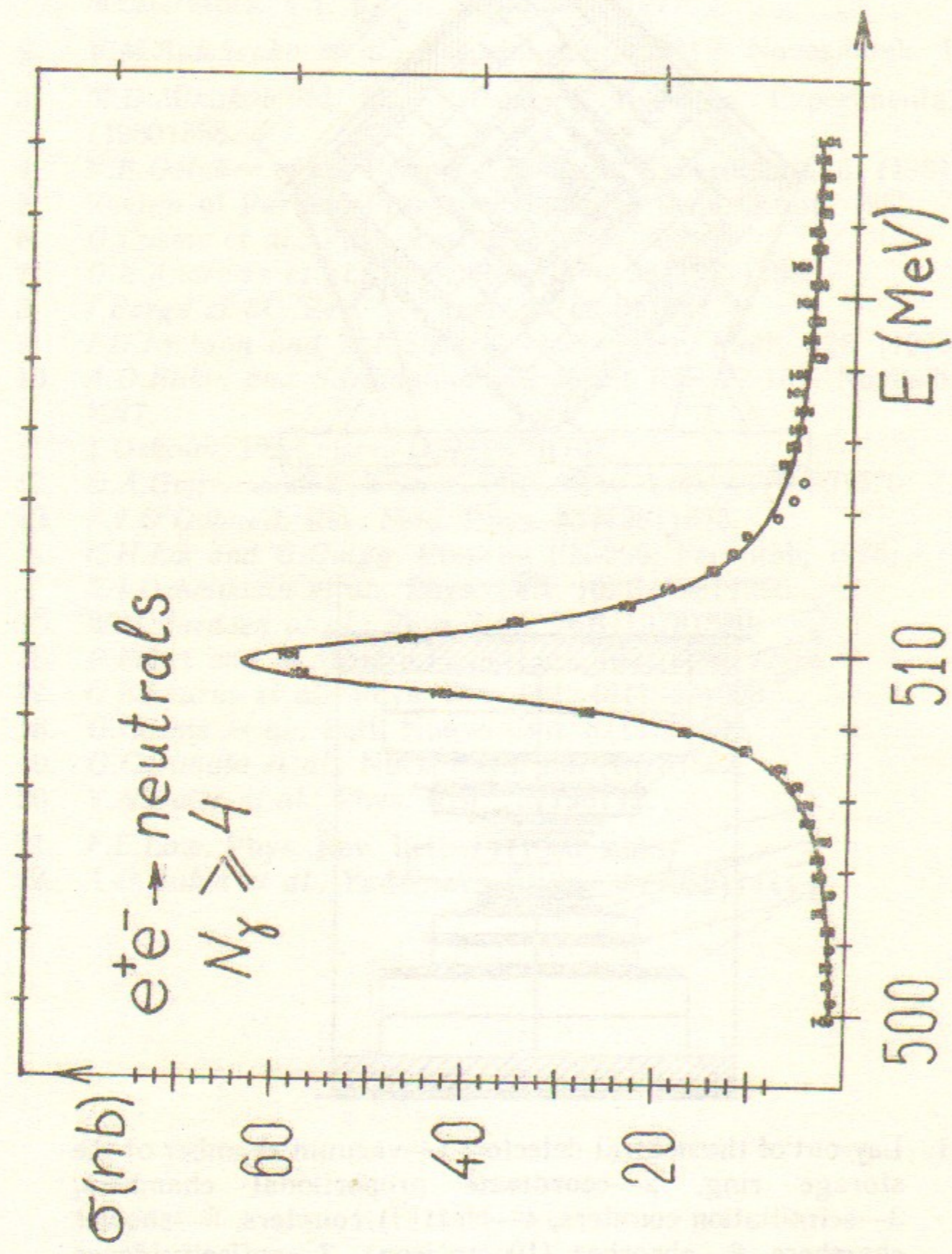


Fig.2. Excitation curve of the Φ -meson in neutral channels.

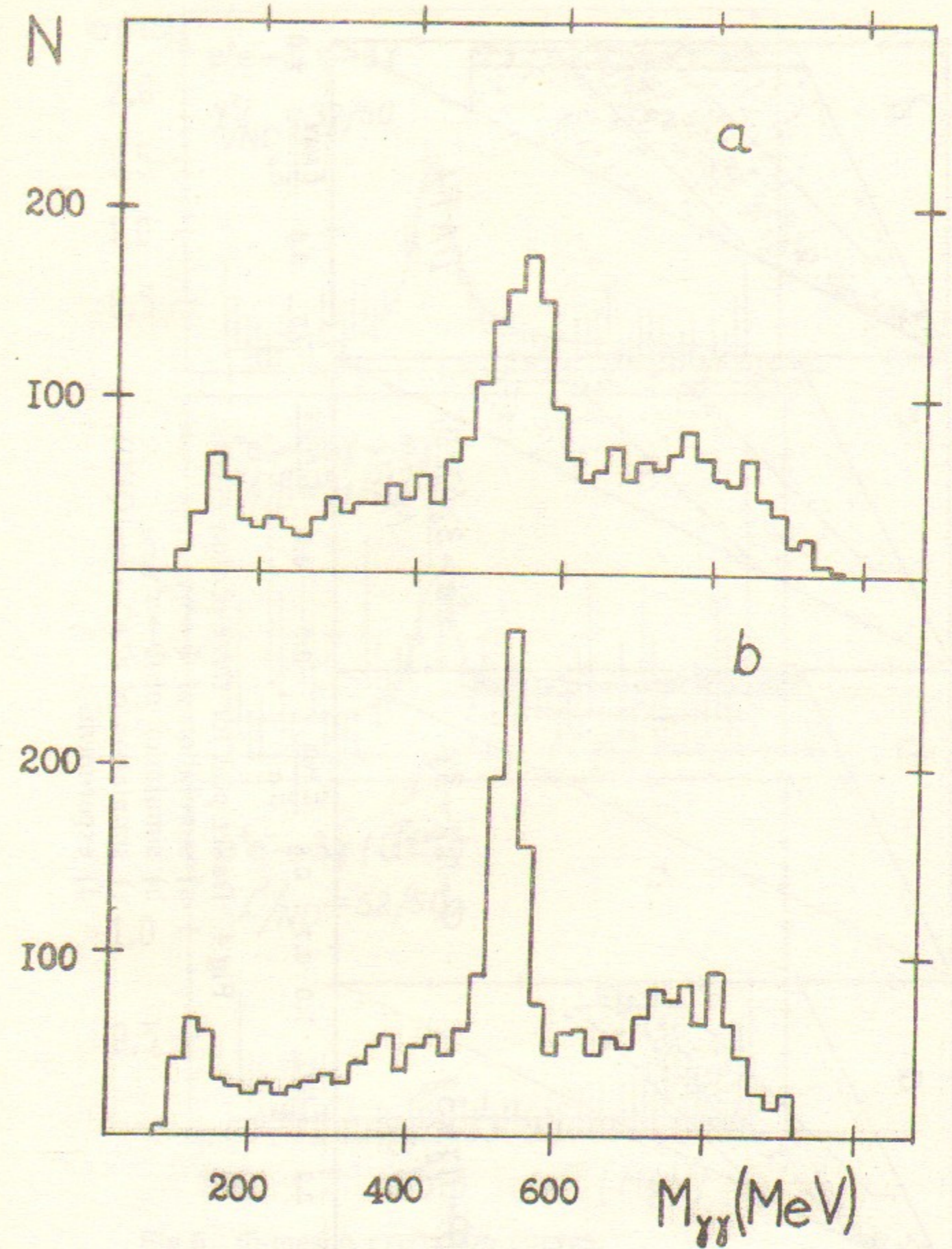


Fig.3. Spectra of effective masses of photon pairs in three-photon events before (a) and after (b) kinematical reconstruction.

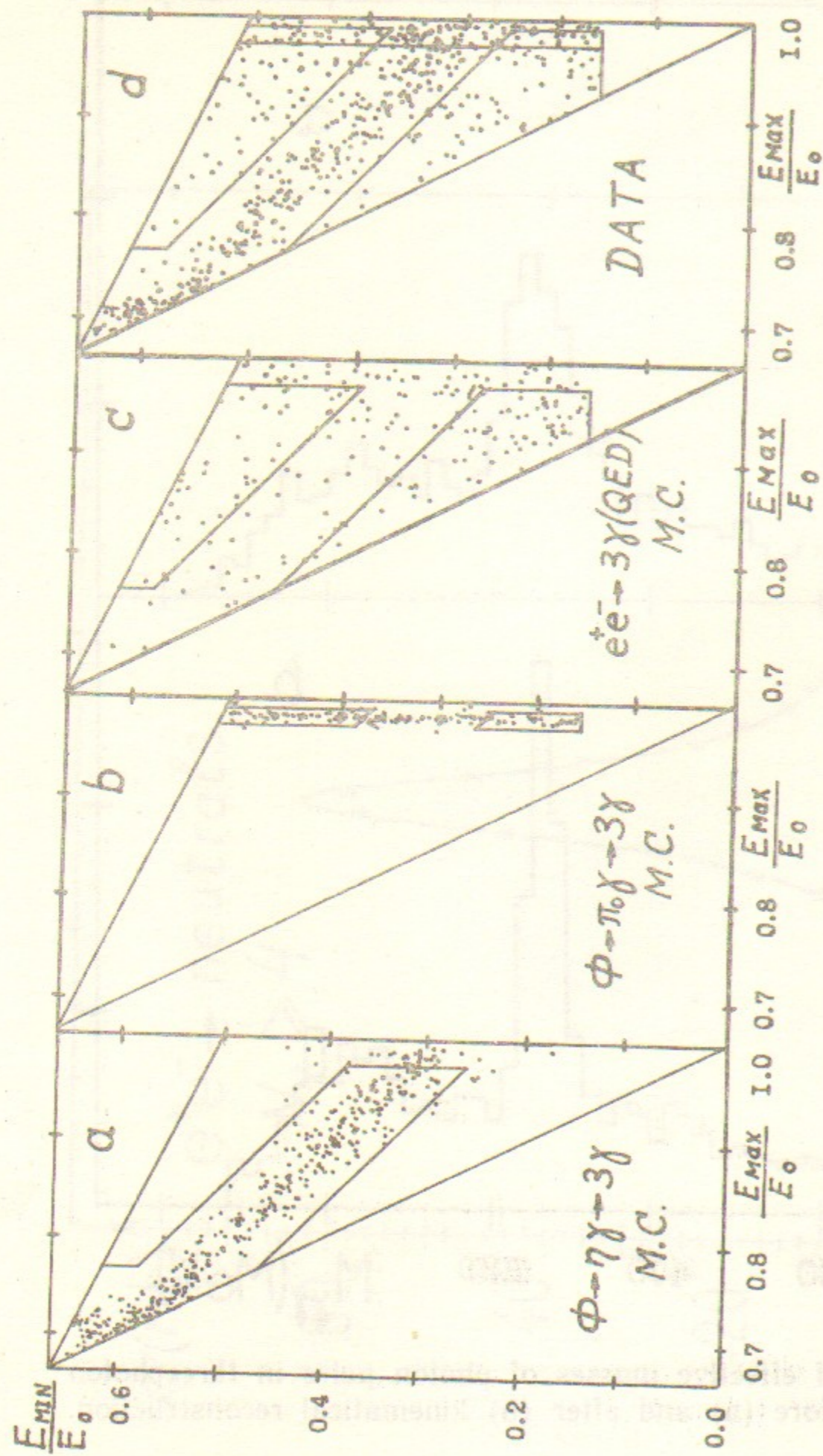


Fig.4. Dalitz plot for three-photon events:

- a) simulation of $\Phi \rightarrow \eta\gamma$,
- b) simulation of $\Phi \rightarrow \pi^0\gamma$,
- c) simulation of $e^+e^- \rightarrow 3\gamma$ (QED),
- d) experiment.

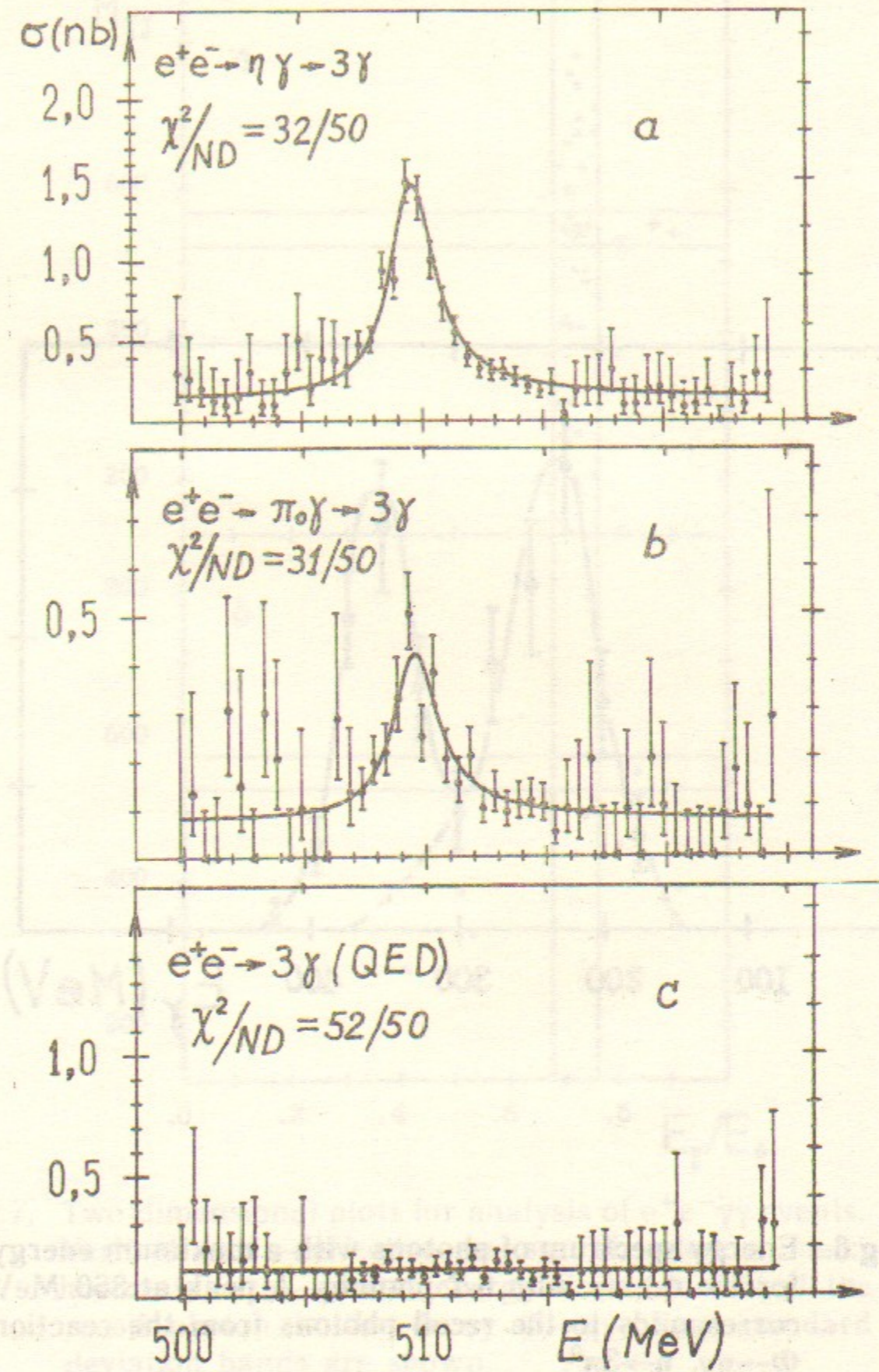


Fig.5. Φ -meson excitation curves:

- a) mode $\Phi \rightarrow \eta\gamma$,
- b) mode $\Phi \rightarrow \pi^0\gamma$,
- c) mode $e^+e^- \rightarrow 3\gamma$ (QED) for comparison.

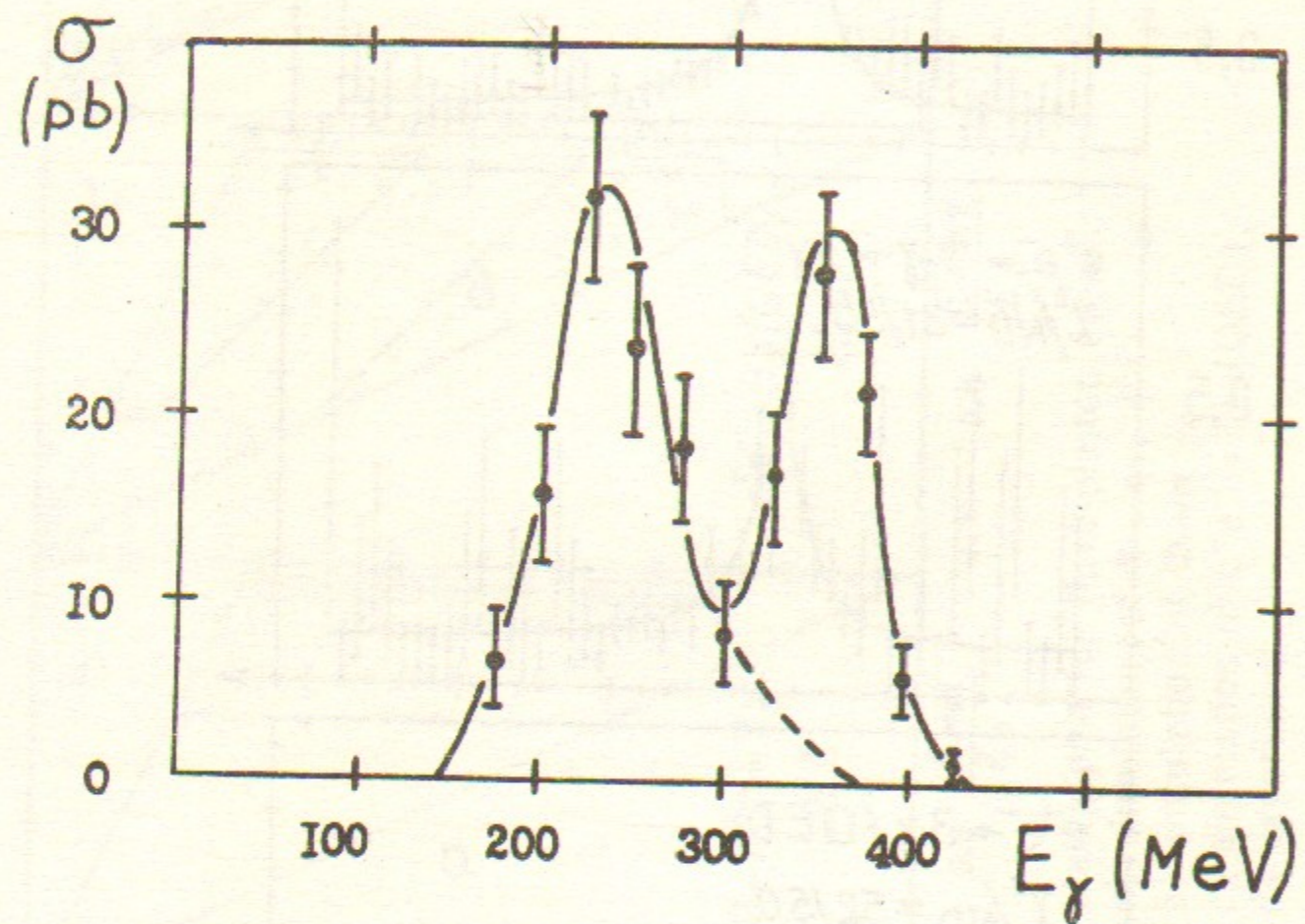


Fig.6. Energy spectrum of photons with a maximum energy for the events with 6-7 photons. A peak at 360 MeV corresponds to the recoil photons from the reaction $\Phi \rightarrow \eta\gamma$, $\eta \rightarrow 3\pi^0$.

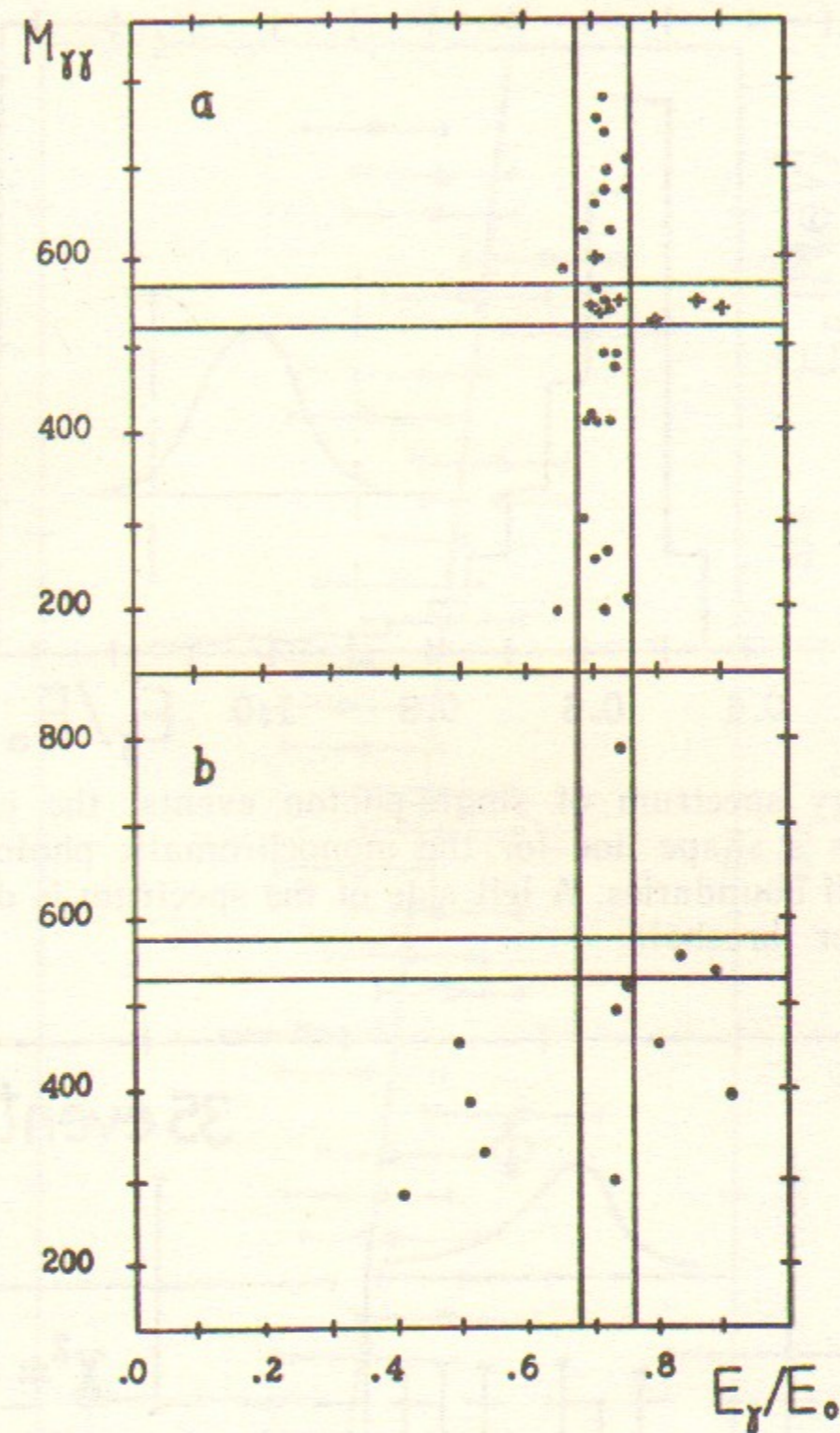


Fig.7. Two-dimensional plots for analysis of $e^+e^-\gamma\gamma$ events. Vertical axis—effective mass of photon pair, horizontal axis—photon energy closest to that of the recoil photon in the decay $\Phi \rightarrow \eta\gamma$. Two standard deviation bands are shown.

- a) Simulation: points—decay $\Phi \rightarrow \eta\gamma$, $\eta \rightarrow e^+e^-\gamma$, crosses—decay $\Phi \rightarrow \eta e^+e^-$, $\eta \rightarrow 2\gamma$,
- b) experiment.

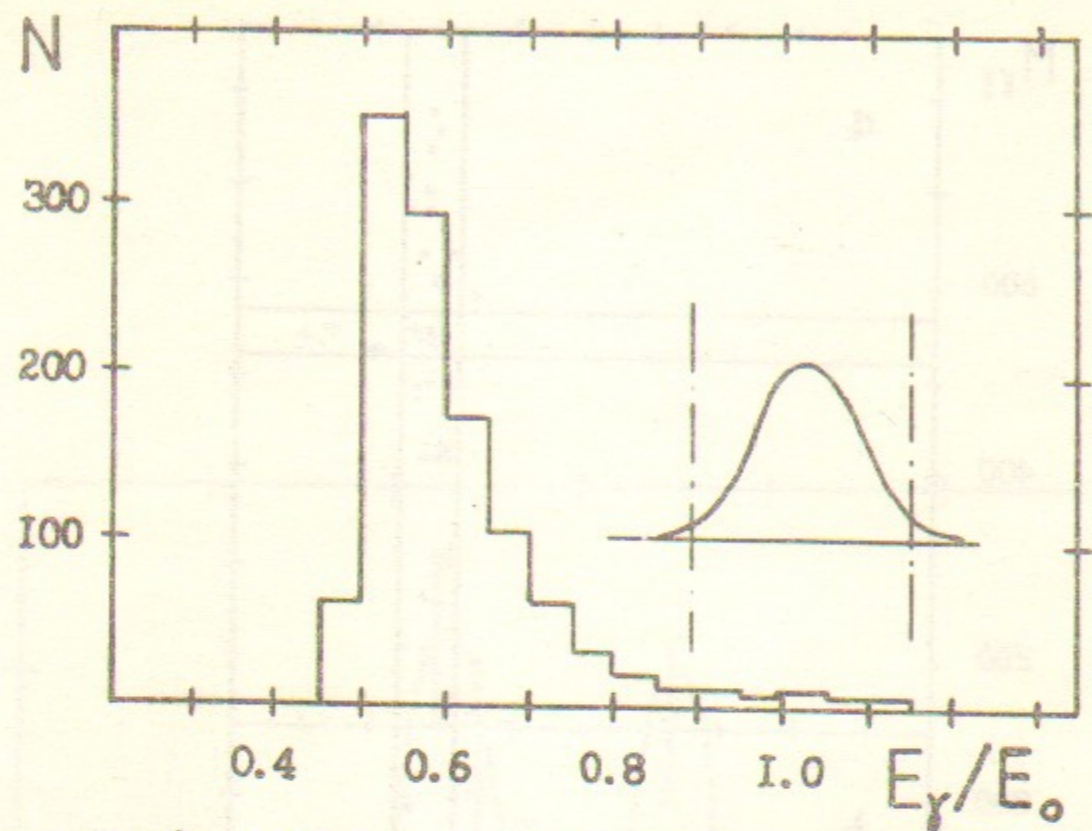


Fig.8. Energy spectrum of single-photon events, the insertion shows a shape line for the monochromatic photons and cut-off boundaries. A left side of the spectrum is due to a trigger threshold.

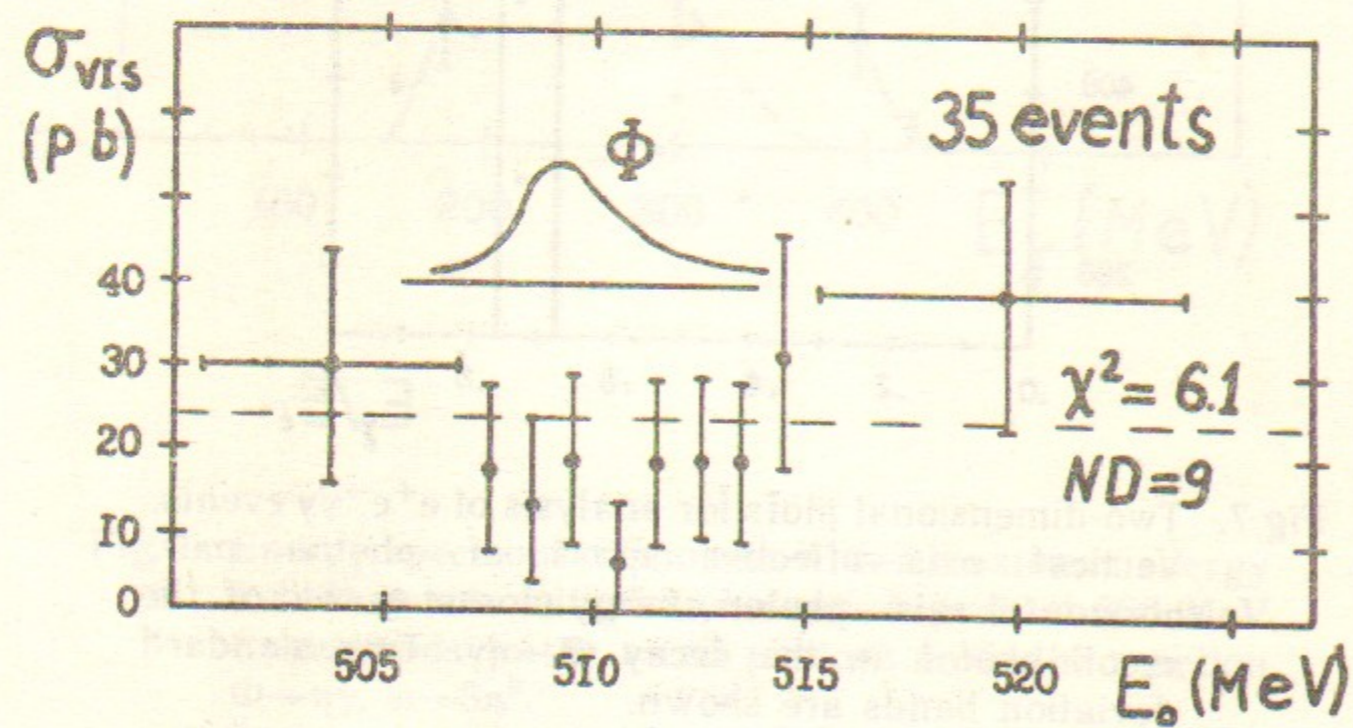


Fig.9. Energy dependence of the detection cross section for hard photons, the insertion shows a position of the Φ -meson resonance.

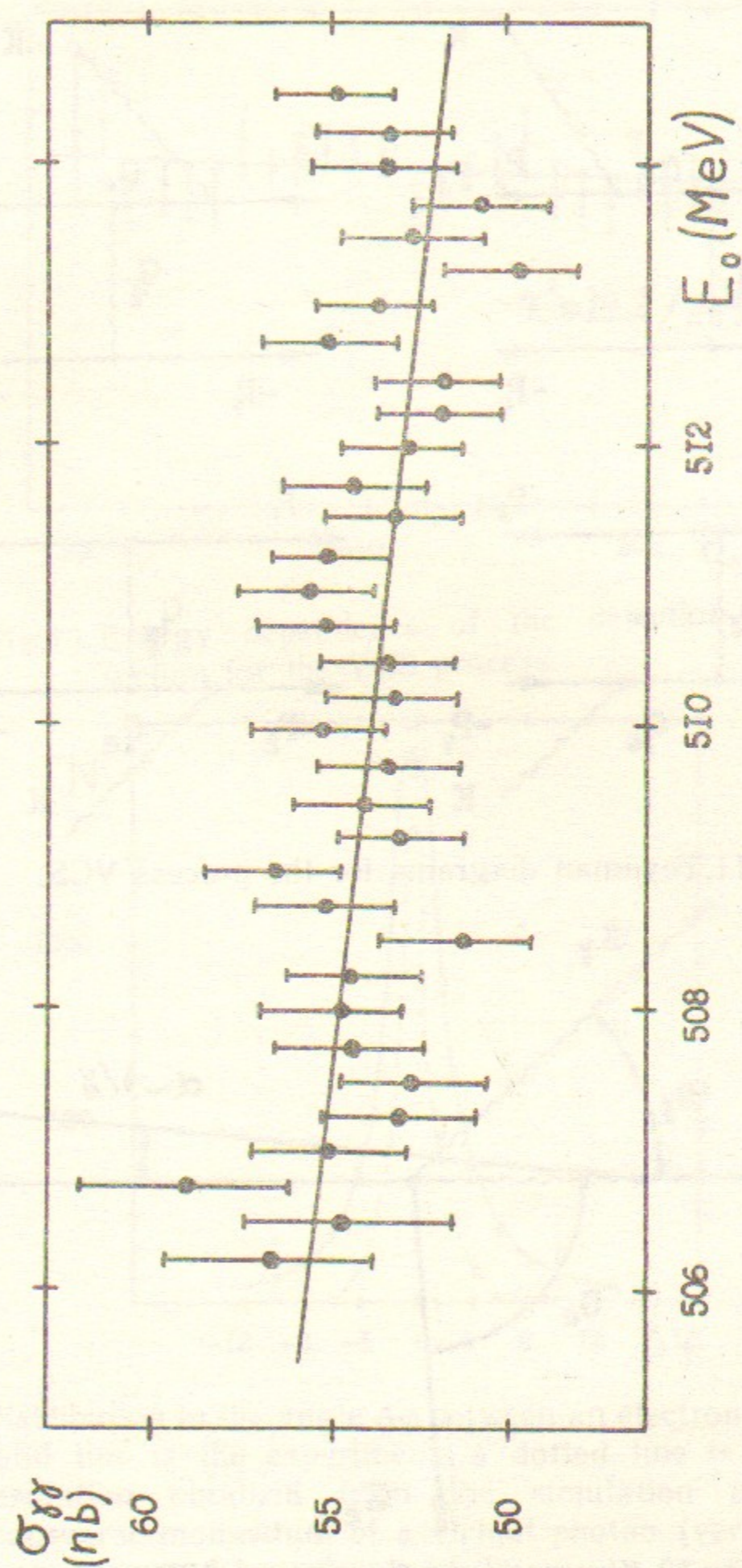


Fig.10. Energy dependence of the detection cross section for the reaction $e^+e^- \rightarrow 2\gamma$.

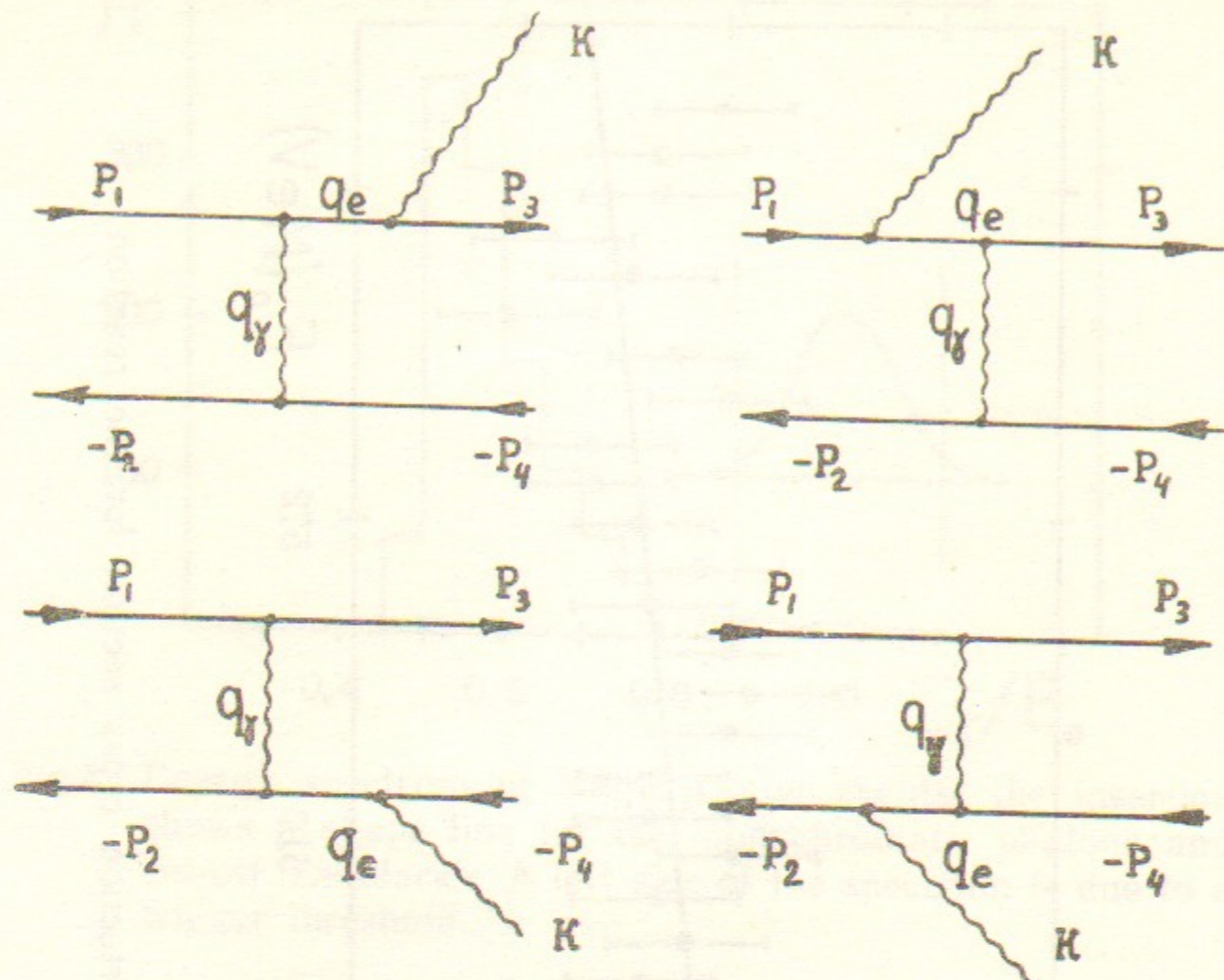


Fig.11. Feynman diagrams for the process VCS.

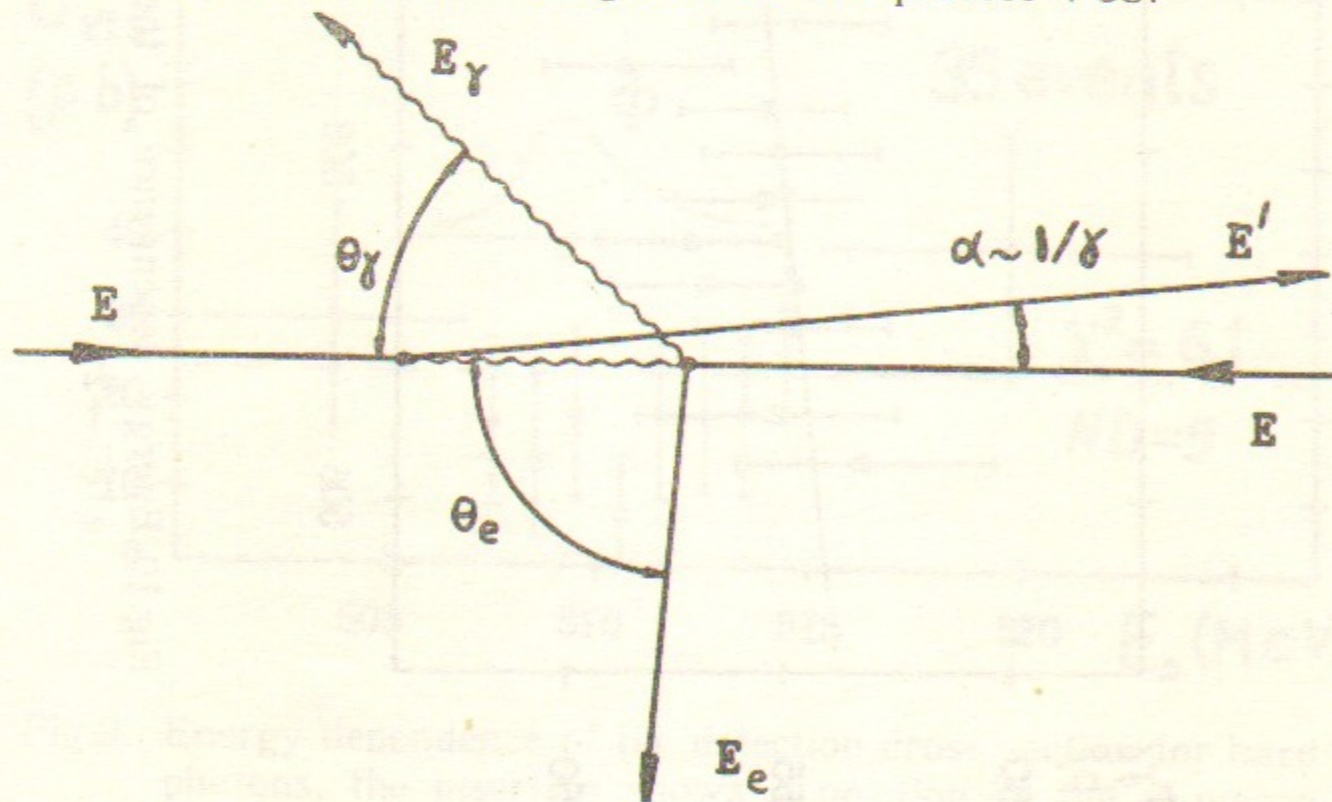


Fig.12. Kinematics of the process VCS.

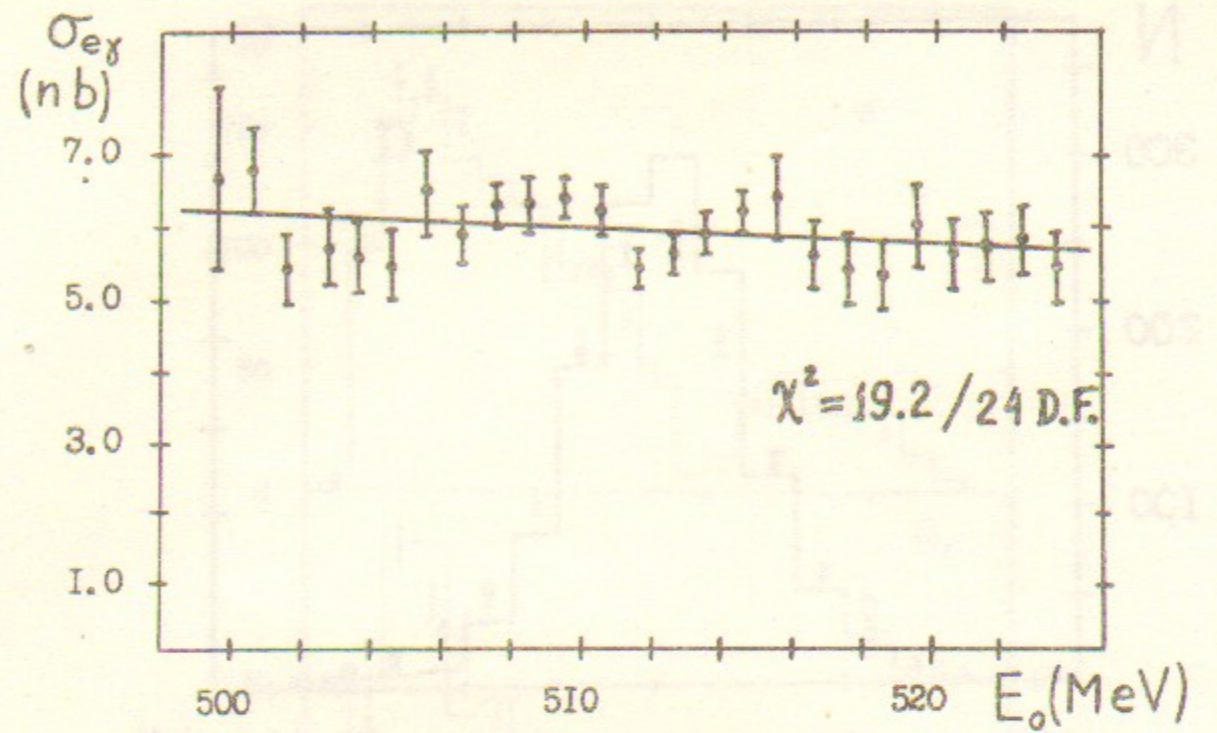


Fig.13. Energy dependence of the detection cross section for the VCS process.

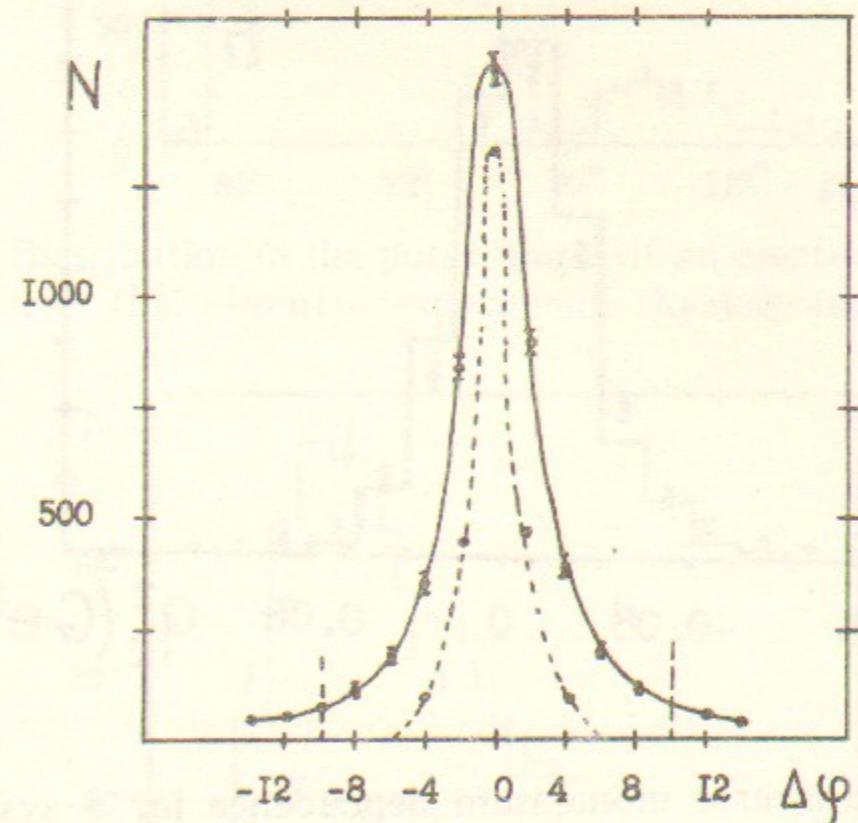


Fig.14. Distribution in the angle $\Delta\phi$ between an electron and photon. A solid line is the experiment, a dotted line is an apparatus resolution obtained from the simulation neglecting the transverse momentum of a virtual photon (vertical scale has been decreased by a factor of 2).

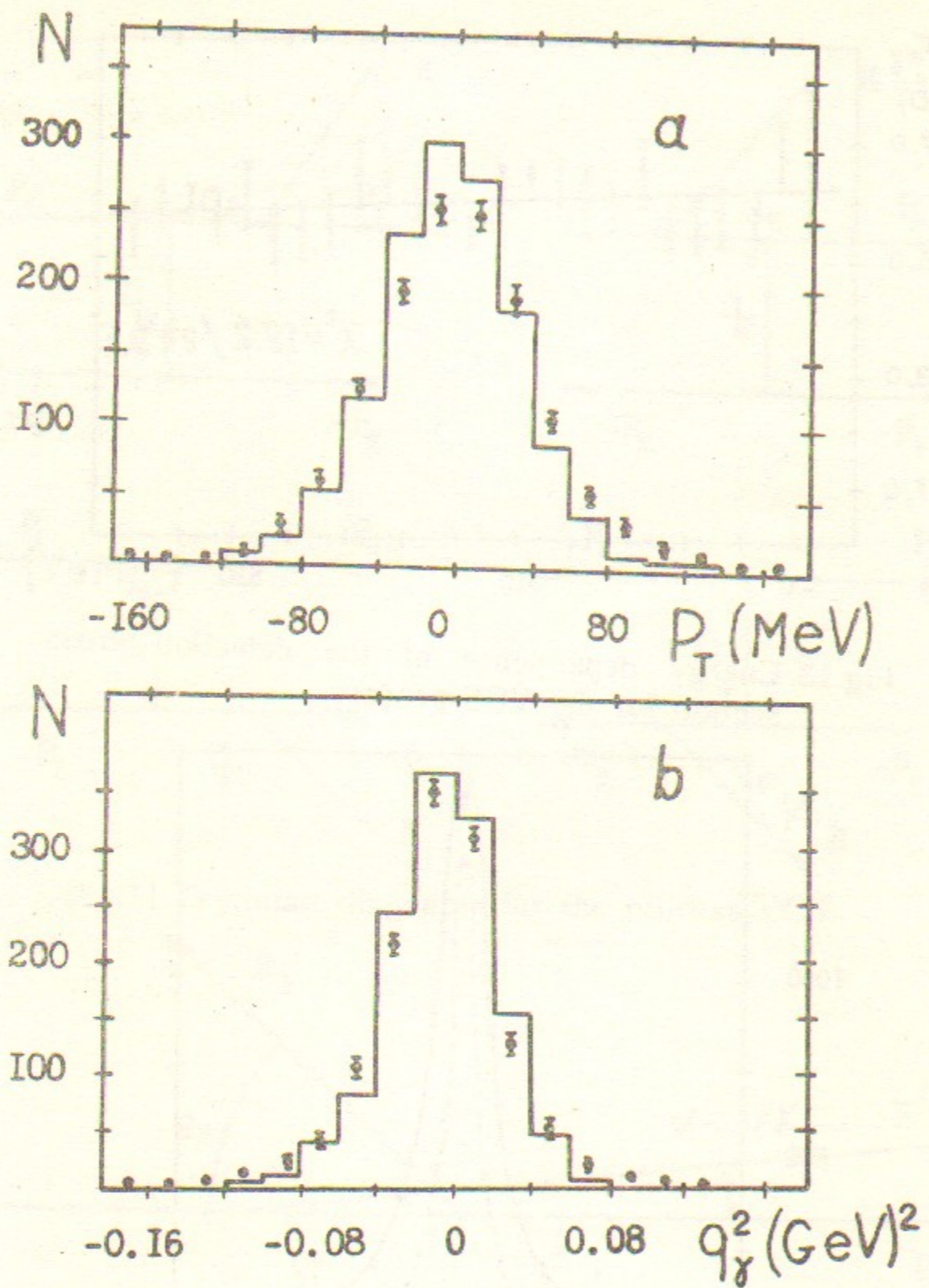


Fig.15. a) transverse momentum dependence for a system electron+photon; b) distribution in the effective mass of a virtual photon. Points—experiment, histogram—simulation (1300 events).

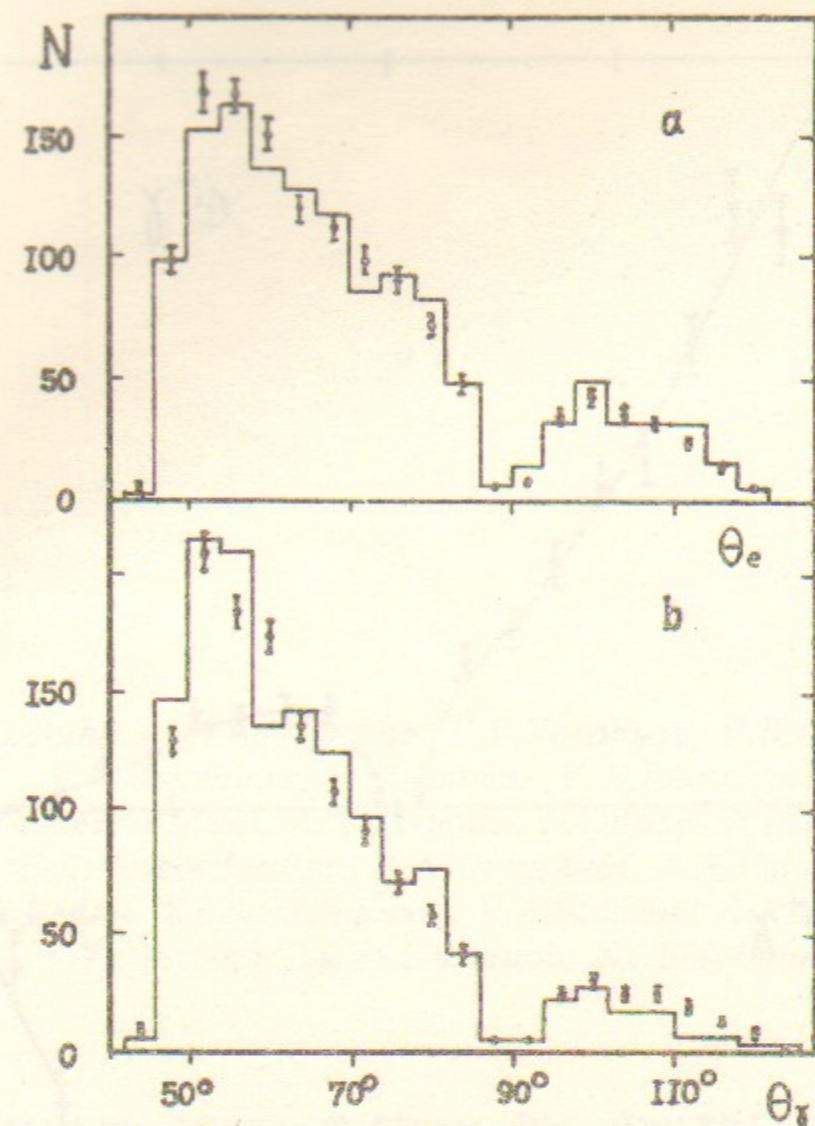


Fig.16. Distribution in the polar angle of an electron (a) and photon (b). Points—experiment, histogram—simulation.

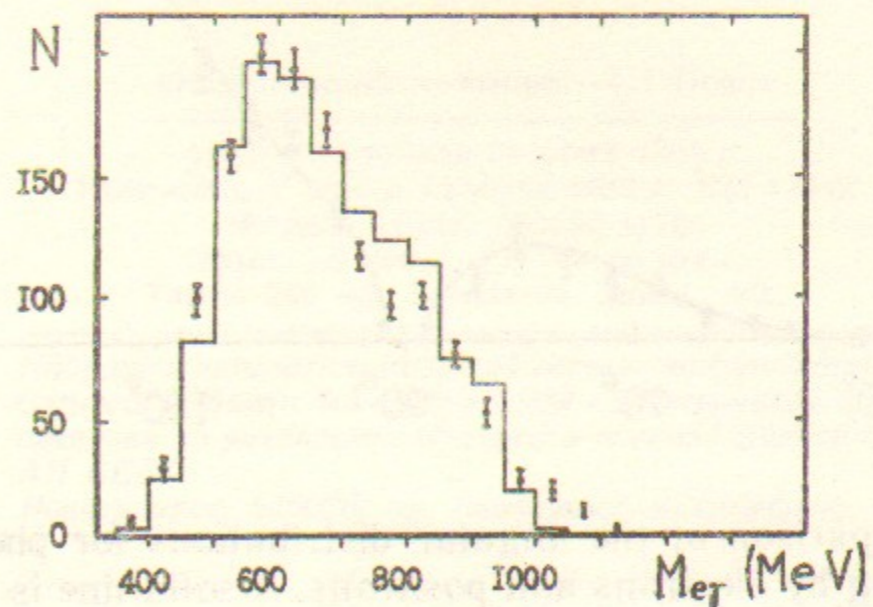


Fig.17. Spectrum of effective masses of electron and photon. Points—experiment, histogram—simulation.

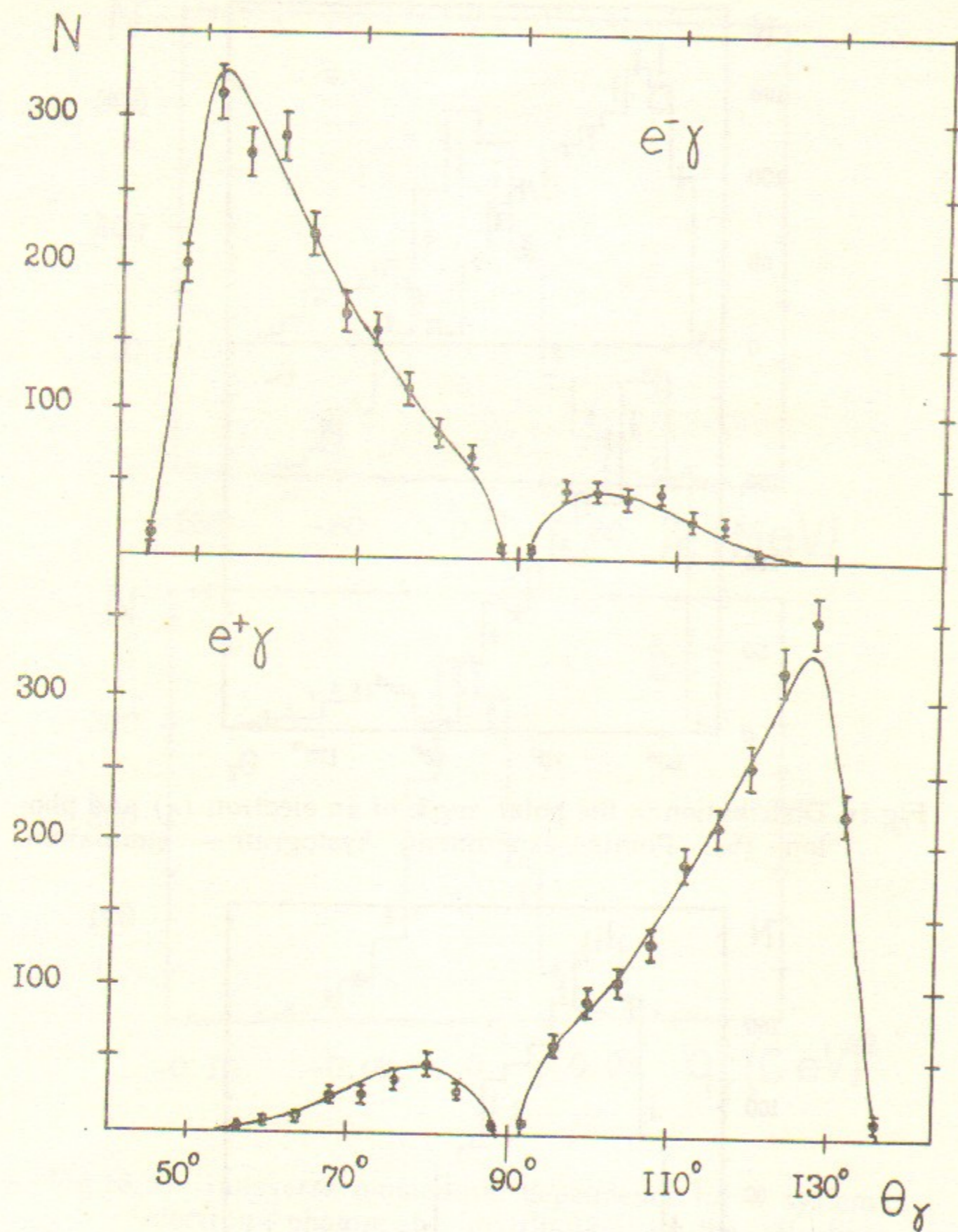


Fig.18. Comparison of the angular distributions for photon scattering by electrons and positrons. A solid line is drawn by hand for better visualization.

*A.D.Bukin, I.B.Vasserman, P.V.Vorobyov, V.B.Golubev,
V.P.Druzhinin, P.M.Ivanov, V.N.Ivanchenko,
G.Ya.Kezerashvili, A.N.Kirpotin, I.A.Koop, A.P.Lysenko,
E.A.Perevedentsev, A.N.Peryshkin, A.A.Polunin,
I.Yu.Redko, S.I.Serednyakov, V.A.Sidorov, A.N.Skrinsky,
Yu.V.Usov, Yu.M.Shatunov, S.I.Eidelman*

**PRELIMINARY RESULTS FROM THE NEUTRAL DETECTOR
AT VEPP-2M**

Ответственный за выпуск—С.Г.Попов

работа поступила 23 июня 1983 г.

Подписано к печати 12 июля 1983 г. МН 17642

Формат бумаги 60×90 1/16.

Объем 1,9 печ.л., 1,5 учетно-издл.

Тираж 290 экз. Бесплатно. Заказ 80.

Набрано в автоматизированной системе на базе фотонаборного автомата ФА-1000 и ЭВМ «Электроника» и отпечатано на ротапринтере Института ядерной физики СО АН СССР,

Новосибирск, 630090, пр. академика Лаврентьева, 11